



Published in final edited form as:

J Orthop Res. 2024 January ; 42(1): 43–53. doi:10.1002/jor.25637.

The Knee Connectome: A Novel Tool for Studying Spatiotemporal Change in Cartilage Thickness

Jennifer Cummings^{1,2}, Kenneth Gao^{1,2}, Vincent Chen¹, Alejandro Morales Martinez^{1,2}, Claudia Iriondo^{1,2}, Francesco Caliva¹, Sharmila Majumdar¹, Valentina Padoia¹

¹Department of Radiology and Biomedical Imaging, University of California, San Francisco, San Francisco, California, USA

²Department of Bioengineering, University of California, San Francisco and University of California, Berkeley Joint Graduate Group in Bioengineering, San Francisco, California, USA

Abstract

Cartilage thickness change is a well-documented biomarker of osteoarthritis pathogenesis. However, there is still much to learn about the spatial and temporal patterns of cartilage thickness change in health and disease. In this study, we develop a novel analysis method for elucidating such patterns using a functional connectivity approach. Descriptive statistics are reported for 1186 knees that did not develop osteoarthritis during the 8 years of observation, which we present as a model of cartilage thickness change related to healthy aging. Within the control population, patterns vary greatly between male and female subjects, while BMI has a more moderate impact. Finally, several differences are shown between knees that did and did not develop osteoarthritis. Some but not all significance appears to be accounted for by differences in sex, BMI, and knee alignment. With this work, we present the connectome as a novel tool for studying spatiotemporal dynamics of tissue change.

Keywords

cartilage thickness; osteoarthritis; knee; analysis methods

1 | Introduction

Osteoarthritis (OA) is a common joint disease characterized by pain and decreased range of motion. OA is one of the most prevalent causes of global disability and is likely to grow more pervasive with increasing life expectancy and obesity rates.¹ The knee is the most afflicted joint, with knee OA accounting for about 85% of global OA burden.²

Corresponding Author: Jennifer Cummings, 1700 4th Street, Suite 201, San Francisco, CA 94158, jenncumings@ucsf.edu, 9177638299.

Author Contributions: V.P. conceived of the study. S.M. and V.P. obtained funding. K.G., V.C., A.M.M, C.I., and F.C. performed data preprocessing. K.G. created preprocessing pipeline figure. J.C. performed analysis and figure generation and wrote the draft of the manuscript. All provided critical feedback on results and approved the final manuscript.

The authors declare no competing financial or non-financial interests.

While growing evidence suggests that OA involves a complex pathogenesis of structural changes to the cartilage, bone, ligaments, and muscles,^{3,4} articular cartilage changes are the most studied feature of OA progression.^{5,6} Early stages of OA are characterized by cartilage changes including increased hydration, proteoglycan loss, and disruption of collagen fibers, while later changes include dehydration and thinning of the cartilage, resulting in denudation of the underlying bone.⁷

Cartilage thickness and volume changes measured with Magnetic Resonance Imaging (MRI) have proven useful in predicting OA progression.^{8,9} However, the exact nature of this relationship remains to be characterized. Studies have shown both cartilage thickening and thinning at different rates and locations of the knee in healthy and diseased subjects.^{10–13} Given the complexity and long timescale of OA progression, it is likely that differences in the length of time between thickness measurements and in disease states between patient groups account for some of these discrepancies. Knees at earlier stages of the disease have shown cartilage thickening and thinning in the medial femorotibial compartment with similar proportions, while later stages are more associated with thinning. This is consistent with animal studies showing that early OA cartilage may appear to thicken as a result of hypertrophy or swelling.^{10,14,15} Cartilage changes have also been shown following anterior cruciate ligament (ACL) injury, a substantial risk factor for developing OA. Overall femorotibial cartilage thickness was found to increase in the 5 years following injury, particularly in the medial femorotibial compartment, but subregional thinning and thickening was observed within the same cartilage plate.¹⁶ A recent study attempted to capture the longitudinal dynamics of cartilage thickness by quantitatively assessing the cartilage thickness trajectories of several knee compartments at 7 timepoints over the course of 8 years.¹⁷ These results indicated that knees with nonstable trajectories, including both net thickening and net thinning, had higher adjusted odds of OA incidence than stable trajectories.

While most studies of knee cartilage thickness have obtained just a few data points from the entire cartilage plate of a bone, usually by measuring at select locations or averaging over a large portion of the surface, growing evidence suggests that spatially localized cartilage thickness changes hold clinical relevance. Cartilage thickness has been shown to vary on the scale of millimeters within the medial and lateral weight-bearing regions of the femur in healthy knees.¹⁸ Another study of healthy subjects reported that the most distal points of femoral condylar cartilage, which engage the tibia most during extension, are thinner than the most posterior points, which engage the tibia during flexion, and that the posterior-medial cartilage is thicker than lateral.¹⁹ Furthermore, evidence suggests that spatial distributions of cartilage thickness grow increasingly variable during OA progression. One study of female subjects demonstrated the most thickening in the peripheral subregions of the central medial femur at early stages of the disease, while knees at later stages showed pronounced thinning throughout the central medial femur.²⁰ Another study associated late-stage OA with thinner cartilage in anterior parts of the medial femoral condyle and thicker cartilage in the posterior condyle.^{21,22} It is likely that spatial variation in cartilage thickness has previously been obscured by the practice of averaging over large areas of cartilage without accounting for spatial differences in geometry and function.²⁰

The objective of this study was to better understand both the temporal and spatial dimensions of knee cartilage thickness change as they relate to osteoarthritis protection and risk factors. Leveraging recent advancements in deep learning, we employed automatic segmentation methods to obtain cartilage thickness measurements from a spatially dense point cloud representation of the femur cartilage for 1418 knees at seven time points over the course of 8 years. We then made use of an analysis method traditionally employed in functional neuroimaging studies, the connectivity matrix, or “connectome”, to explore the statistical relationships between cartilage thickness trajectories at each subregion. With this tool, we aimed to elucidate patterns of functional connectivity in the knee joint that may serve as biomarkers of healthy or pathological knee aging.

2 | Methods

2.1 | Study Population and Data Selection

The Osteoarthritis Initiative (OAI) data set was used for this study. This is a multi-center prospective longitudinal study.²³ The study enrolled 4,796 participants with or at risk of OA in the United States between February 2004 and May 2006. OAI subjects were monitored across 12 time points, from an initial baseline visit to a final 108 month visit.²³ Out of these 12 time points, MRI scans were performed at seven time points [0,12,24,36,48,72,96] months, resulting in an imaging span of eight years 0–96 months. Demographic data such as age, body mass index (BMI), and sex were also recorded during each visit. Kellgren-Lawrence (KL) grading was performed by trained musculoskeletal radiologists on radiographs of both knees at the enrollment visit, 12-month, 24-month, 36-month, and 48-month for all the participants in the OAI. KL grading depicts structural abnormalities and is the accepted standard for OA diagnosis as well as the most widely used structural outcome in epidemiological studies and clinical trials.²⁴ OAI MRI imaging protocol includes a 3D double-echo steady-state (3D-DESS,3T Siemens) which is the only sequence used for cartilage thickness biomarker extraction. MRI parameters included: TR/TE 16.2/4.7; FOV, 14 cm; matrix, 307×384; bandwidth, 71 kHz; and image resolution, [0.365, 0.456, 0.7] mm).

From the total of 9,592 3D-DESS knee MRIs acquired from bilateral examination of 4,796 participants at the baseline time point, we selected knees that did not have a diagnosis of radiographic OA at baseline (KL grade < 2) and for which data was available for all follow-up visits. With these inclusion/exclusion criteria we obtained a data set of 1418 knees (1035 unique subjects). On the total of 1418 knees included in this study, 232 (16%; at least one knee from 218 unique subjects) had incident radiographic OA (KL grade > 1) over the course of the study, resulting in a control group of 1186 knees and an OA incidence group of 232. Demographics at baseline for the control and OA incidence groups are shown in Table 1.

2.2 | Knee Alignment Classification

Femur–tibia angle (FTA) data on baseline radiographs were available for a subset of the knees in the study (n = 683, 45.9% of all knees in study), consisting of 454 knees that did not develop OA and 229 knees that did. These data were used to classify the subset into varus, neutral, and valgus alignment groups. FTA data were first translated to hip-knee-ankle

(HKA) angle equivalent using a previously proposed formula:²⁹ $HKA_{eq} = FTA * 0.98 + 4.0$. The following thresholds were then used to define groups: Varus = $HKA_{eq} < -2^\circ$; Neutral = $-2^\circ < HKA_{eq} < 2^\circ$; Valgus = $HKA_{eq} > 2^\circ$. Varus and valgus alignment for knees within each subset of the control and OA incidence groups are shown in Table 1.

2.3 | Image Processing

A bone and a cartilage segmentation model ensemble based on multiple 2D and 3D V-nets were trained on 72 and 148 manually annotated 3D-DESS volumes to automatically segment the femur, tibia, and patella bones and corresponding cartilage. The two models were extensively validated and tested obtaining Dice Score Coefficient (DSC) equal to $98.0\% \pm 0.32\%$, $98.0\% \pm 0.26\%$, and $96.4\% \pm 0.70\%$ for the femur, tibia, and patella bone respectively. The cartilage segmentation test dice scores were $90.0\% \pm 0.74\%$, $88.6\% \pm 1.3\%$, and $85.7\% \pm 2.5\%$ for the femoral, tibial, and patellar cartilage respectively. Implementation details and evaluation strategies are reported in previously published work^{17,25,26} and summarized in Figure 1. The trained models were used in inference to segment all the 3D-DESS volumes available in OAI (45,789); cartilage thickness maps were obtained from the segmented masks using a distance transform method previously proposed¹⁷. Automatic evaluation results were compared with the ones performed manually, which are publicly available on the OAI website (N=4,299). We observed strong correlations and mean absolute errors within the voxel resolution. Pearson r values ranged between 0.850 in central Lateral Femur and 0.955 in Lateral Tibia; average absolute difference ranged between 0.108 mm in Medial Tibia and 0.143 mm in central Lateral Femur.

A normal vector spanning from each point in the bone surface was used to sample the overlying cartilage thickness by averaging the thickness values at all skeleton points within a radius of 0.729 mm, empirically set to double the in-plane pixel resolution. With this procedure we obtained dense thickness maps for each knee and each time point encoded in a triangulated mesh of a variable number of vertices spanning between 46816–124422. All meshes were then registered to a single atlas bone surface selected to match the average demographic distribution of the used data set. The landmark matching strategy used in this study was based on the one proposed by Lombaert, H. et al.²⁷ The maximum and minimum local curvatures were used for coupling homologous points on two surfaces. Both these features were locally defined on the surfaces and used to identify the landmark matching solved using Coherent Point Drift.²⁸

2.4 | Knee Connectome

We created a parcellation of the femur cartilage by dividing the cartilage mask into 2 equally spaced sections along the medial-lateral axis and 3 equally spaced sections along the anterior-posterior axis, with the middle third labeled as the weight-bearing section. The medial and lateral sides were further divided along the medial-lateral axis into 5 subsections each. 3 of these subsections fell out of the cartilage mask due to the curvature of the bone, including the outermost subregions of the anterior medial and anterior lateral compartments and the most central subregion of the posterior medial compartment, resulting in 27 subregions total (4–5 subregions per compartment). The resulting atlas is shown in Figure 2. Cartilage thickness trajectories were calculated for each subject for each of the 27

subregions by averaging the thickness measurements at all vertices within each subregion at each time point.

Pearson correlation coefficient r was used to represent the similarity between each pairwise combination of 27 time series, resulting in a correlation matrix, or connectome, with 729 entries for each subject. The connectome generation process is represented in Figure 3. We consider the r value a representation of functional connectivity between a pair of subregions and thus refer to each entry of the connectome as a “connection”. Group average connectomes were obtained by averaging across connectomes of all subjects within a given group, meaning that each entry in the average matrix is an average of r values at that entry across all group members (e.g., 1186 knees in the average healthy control group). As the connectome is a symmetric matrix, only the lower triangle was considered in analysis and is shown in figures.

2.5 | Statistical Analysis

The aim of our analysis was to investigate whether the connectome would reveal spatiotemporal patterns of cartilage thickness change that are associated with OA protection or risk factors. We first sought to identify consistent patterns in the cohort of subjects that did not develop OA over the course of the study. We averaged connectomes across all healthy knees to obtain group-level descriptive statistics. We then separated connectomes from healthy knees into groups defined by sex and BMI and used the two-sample t -test to evaluate differences between these groups. A BMI ≥ 30 was considered high when dividing control subjects into high and low BMI groups for comparison. Finally, we compared the connectomes of knees that remained control throughout the study with those that developed OA. Partial correlation was used to control for demographic differences including sex, BMI, and knee angle when comparing control and OA incidence groups within the subset of knees for which knee angle data were available. Where applicable, mean r scores are reported as [Mean Positive R; Mean Negative R], indicating that means were obtained over positive correlations and negative correlations separately. Bonferroni correction was applied to control for multiple comparisons, resulting in a p -value threshold of $1.42e-04$.

3 | Results

3.1 | Features of Healthy Knee Connectome

As a first aim, we report the key descriptive features of the average connectome of the 1186 knees that did not develop OA during the 8 years of observation (Figure 4). We consider the average control connectome a model for the spatial-temporal relationship of cartilage thickness longitudinal changes related to healthy aging.

The first feature of note is that intracorrelations, meaning the correlations between different subregions within a region, are stronger than intercorrelations, the correlations between subregions of different regions (Figure 4A). The mean r for positive and negative intracorrelations is [0.42; -0.17], while mean r for intercorrelations = [0.14; -0.07].

A second notable feature is that, within the weight-bearing and posterior intracorrelations, we observe weak to moderate negative correlations in addition to the more expected strong

positive correlations (Figure 4B). Mean r for weight-bearing medial intracorrelations = [0.44; -0.17]; weight-bearing lateral intracorrelations = [0.45; -0.22]; posterior medial intracorrelations = [0.27; -0.20]; posterior lateral intracorrelations = [0.38; -0.09]. While the average of negative correlations is just moderate, this was observed to be a consistent pattern on the control connectome. This observation means that the cartilage thickness trajectory of different regions can diverge, but at a synchronous rate: while one region is thinning over time another appears to be thickening.

Third, we observe that associations between thickness trajectories in the anterior and weight-bearing regions tend to be stronger in the medial side than the lateral side: Medial anterior vs. weight-bearing intercorrelations = [0.30; -0.07]; Lateral anterior vs. weight-bearing intercorrelations = [0.17; -0.05] (Figure 4C). Finally, we show a consistent anticorrelation pattern between medial and lateral weight-bearing regions: Medial vs. lateral intercorrelations = [0.17; -0.10] (Figure 4D).

3.2 | Population differences within control group

Comparing male and female subjects, we find 38 statistically significant connection differences (p values = $2.94e-11$ – $1.22e-04$) (Figure 5A–C). Of these, 55.3% involve the anterior medial region, with anterior medial intracorrelations comprising 15.8% of all significant connections, and 31.6% involve the anterior lateral region. Nearly all significant connections involving the anterior medial and lateral regions have a positive mean for females, apart from one connection between the anterior medial region and weight-bearing medial region, which is weakly negative. 7 of these same connections have a negative mean in the male population: 2 between anterior lateral and weight-bearing lateral, 2 between anterior lateral and anterior medial, 1 between anterior medial and posterior lateral, 1 between anterior medial and weight-bearing lateral, and 1 between anterior medial and weight-bearing medial. This includes the one connection that is negative for females, for which the male mean is more strongly negative. 26.3% of the significant connections involve the weight-bearing medial region, and 39.5% involve weight-bearing lateral. 2 of the 3 significant weight-bearing lateral intracorrelations have a negative mean for both groups, while the other is positive for both. Connections involving posterior medial and lateral regions comprise 7.9% and 13.2%, respectively. 1 is a posterior lateral intracorrelation, which is weakly positive for both on average, but stronger for the female group. There are 2 significant connections for which females have a negative mean and males have a positive mean: 1 between weight-bearing medial and weight-bearing lateral, and 1 between posterior medial and weight-bearing lateral. Of all connections which are positive on average for both groups, 55.5% are more strongly positive for the female group. For all connections that have a negative mean for both, the male mean is more strongly negative.

Comparing the connectomes of the high and low BMI groups, we find two statistically significant differences (p values = $3.03e-05$ – $5.22e-05$) (Figure 5D–F). Both involve the weight-bearing lateral region. One is with the anterior medial region and has a positive mean for the low BMI group and negative for the high BMI group. The other is with the posterior medial region and is weakly negative on average for the low BMI group and positive for the high BMI group.

3.3 | Control vs. OA Incidence Groups

When comparing the control and OA incidence groups, there are 20 significantly different functional connections (p values = $4.07e-14$ – $1.35e-04$) (Figure 6A–C). After controlling for confounding variables (sex, BMI, age, and knee alignment), there are six remaining statistically significant connections (p values = $5.02e-08$ – $1.23e-04$) (Figure 6D). 66.7% of these involve the weight-bearing medial region, with weight-bearing medial intracorrelations comprising 33.3% and the other half involving intercorrelations with the weight-bearing lateral region. Of the two remaining significant connections, one is between weight-bearing lateral and anterior lateral regions, and the other is a posterior medial intracorrelation. 4 of the 6 connections have a positive mean for both groups, 3 of which are more strongly positive for the control group than the OA incidence group. One connection between the weight-bearing medial and weight-bearing lateral regions has a negative mean for the OA incidence group and positive for controls, while one weight-bearing medial intracorrelation has a negative mean for the control group and positive for the incidence group.

4 | Discussion

In this study, we present the first application, to our knowledge, of the connectome as a tool for studying longitudinal cartilage thickness changes in the knee.

Consistent correlation patterns are seen in the connectomes of healthy control subjects, which we present as potential biomarkers of healthy joint aging. We note that these features are evident when averaging across all 1186 healthy knees, supporting the consistency of these results. The trajectories of subregions within a given functional region are strongly correlated. This is an expected feature, as it is not surprising that adjacent subregions progress more synchronously than regions located in portions of the articular surface that might be loaded or engaged differently during movements such as knee flexion vs standing weight-bearing.

One notable aspect is the presence of negative correlations, meaning that one subregion must be thinning while another is thickening. While we are not the first to report the presence of both thickening and thinning within the same joint,^{10,30} our findings add another dimension to this analysis, suggesting a functional relationship underlying these changes. Importantly, the use of correlation as our main metric provides a means of capturing temporal dynamics that have not previously been studied. When treating the trajectory of measurements as a raw time signal, we observe waveforms indicating fluctuations in cartilage thickness between each time point. The presence of negative correlations between these time series suggests that these fluctuations are not simply capturing intrinsic changes in the subject's state (e.g., differences in hydration at time of scan), which would likely result in global cartilage thickness changes, but are actually representing relationships in which thinning in one spatial location on the cartilage surface is accompanied by thickening in another.

There are several potential explanations for this. One hypothesis is that our results represent a process by which the femur cartilage maintains homeostasis; if one part of the cartilage is always thickening when another is thinning, there is no widespread cartilage degeneration. The causes of this could be mechanical (e.g., shifts in weight distribution leading to

changes in compression), biological (inflammation at one site recruiting resources from another), or a combination of the two. It is well known that early stages of OA are characterized by increases in cartilage thickness, which have been attributed to an influx of water to the extracellular matrix following increases in aggrecan production by proliferating chondrocytes.^{2,49} It is possible that the dynamics we report here represent transient instances of synthetic chondrocyte activity which serve to repair tissue without initiating long-term inflammation and degradation.³¹

Furthermore, most negative correlations exist between subregions that are more central to the knee midline and ones located on the periphery. Previous studies have shown topographical differences on a molecular level within knee cartilage, with peripheral regions of the tibial plateau exhibiting a more organized matrix of collagen fibers and smaller, flatter chondrocytes oriented tangentially to the surface.³² These results suggest that local cartilage structure develops in response to the direction of maximum load it receives, which will vary along the cartilage surface as a function of underlying bone geometry. It is thus possible that our results capture spatial variations in cartilage response to changes in the global state of the joint (e.g., a change in physical activity patterns eliciting different responses in different anatomical locations depending on variations in load experienced locally). The consistency of these patterns among the control group over an eight-year span suggests that this pattern plays a role in maintaining joint health.

Female sex and obesity are two strong risk factors in developing OA.³³ By investigating the connectome differences between these groups in the control population, we sought to determine whether patterns of cartilage thickness changes exist that are specific to a given demographic. When comparing female and male connectomes within the control group, we see several significant differences, most of which involve the anterior and weight-bearing regions of the femur. We also note the presence of weaker positive correlations and stronger negative correlations in men than women, indicating more widespread similarity in cartilage thickness trajectories in women (i.e., more subregions thickening or thinning simultaneously). Several sex differences have been suggested as possible factors leading to higher OA risk in women that may also relate to the differences seen here. Women tend to have thinner cartilage in the knee joint as well as smaller cartilage volume and surface area.³⁴ Relatedly, female sex is associated with a thinner patella and femur and a smaller lateral tibial condyle compared to the medial tibial condyle.^{35,36} Sexual dimorphisms in the molecular structure of cartilage may also play a role. It has been shown that estrogen receptors exist in articular cartilage and that estrogen replacement therapy may protect against the development of OA, indicating that hormonal differences impact cartilage properties.^{36,37}

Interestingly, we don't see much difference between the connectomes of high and low BMI subjects within our control group. This suggests that subjects with higher BMI who do not develop OA exhibit similar functional cartilage properties to their lower BMI counterparts. It is worth noting that Pearson's correlation is a scale-invariant metric, meaning that it is not influenced by overall cartilage thickness itself but by the amount a change in one time series can be predicted by change in another. Thus, while higher BMI has been associated with changes in overall cartilage thickness related to increased joint loading,^{38,39} the similarities

we show here between high and low BMI control subjects may represent a protective mechanism that is not based on absolute cartilage thickness but on cartilage dynamics. Growing evidence suggests that the link between obesity and OA, and the etiology of OA more generally, is not simply attributed “wear-and-tear” in the joints but involves a complex interaction of inflammatory and metabolic processes that may be heightened in high-fat environments.⁴⁰ Furthermore, it has been suggested that knee angle plays a large role in mediating the impact of BMI on OA progression.^{41–43} Finally, we acknowledge that alternative metrics to BMI, such as waist circumference and body fat percentage, may provide more information in parsing the relationship between weight and knee OA, although previous studies have found such variables to be highly correlated and affirmed the role of BMI in risk prediction.^{44,45}

We observe several significant differences between the connectomes of healthy knees and those that developed OA, many of which involve connections where the control group exhibits stronger negative correlations than the OA incidence group. Much of this statistical relationship appears to be accounted for by the confounding variables of sex, BMI, and knee alignment, although the reduction in subject number when excluding subjects without knee angle data may also decrease the level of statistical power. Our results suggest that cartilage thickness changes within the weight-bearing region of the femur play a particularly important role in OA development. This agrees with previous literature.⁴⁶ One particularly relevant study found that cartilage volume loss in OA subjects after 24 months was most pronounced in the central (weight-bearing) areas of the medial and lateral condyles, with medial volume loss exceeding lateral.⁴⁷ Interestingly, our results point to a stronger correlation between medial and lateral weight-bearing compartments in the control group compared to OA, suggesting that asynchronous or imbalanced change between the two weight-bearing compartments may play a role in OA development. Similarly, higher absolute intracorrelation within the medial weight-bearing region in the control group may indicate an adaptive functional relationship between subregions that is less present in the OA group.

Importantly, we acknowledge that the collection of knee MRI images over such a long time scale and at such high resolution is not feasible nor warranted for clinical use.⁴⁸ However, our results suggest that a consistent pattern of both thinning and thickening within the same knee cartilage may be a trademark of healthy knee aging, which may provide a new outcome metric for the development of OA therapies. It would be valuable to investigate whether such dynamics are observable on a shorter time scale. Another limitation of our study is the use of only baseline demographics, and future study might involve a more in-depth analysis of knee cartilage changes in relation to changes in knee angle over time as well as associated factors such as BMI, injury incidence, and pain scores. Future research may also involve development of a more complex, patient-specific cartilage parcellation scheme that accounts for anatomical landmarks such as meniscus coverage.

In summary, we present the connectome as a novel analysis method for studying spatiotemporal dynamics of tissue change and demonstrate its utility when applied to knee cartilage thickness trajectories. A key conclusion of this study is that finer-grained parcellation of cartilage reveals differences in longitudinal thickness trajectories that

may hold clinical relevance. Consistent patterns are observed in the cartilage thickness trajectories of healthy knees over the span of eight years which are characterized by the presence of synchronous thickening and thinning within different subregions of the same femur surface. Male and female subjects within the control group exhibit highly divergent patterns of cartilage thickness change. Differences are also found between knees that did and did not develop OA over the course of the study, most of which involve the weight bearing regions of the femur. Sex, BMI, and knee alignment account for some but not all significant differences.

Acknowledgments

This work was supported by research grants from the National Institute of Health (NIH):

1. Deep Learning for Characterizing Knee Joint Degeneration Predicting Progression of Osteoarthritis and Total Knee Replacement, Grant/Award number: NIH/NIAMS R33AR073552
2. Multidimensional MRI-based Non-Euclidean Deep Learning to Study Osteoarthritis, Grant/Award number: NIH/NIAMS R00AR070902

References

1. Hunter DJ, March L, Chew M. Osteoarthritis in 2020 and beyond: a Lancet Commission. *The Lancet*. 2020;396(10264):1711–2.
2. Hunter DJ, Bierma-Zeinstra S. Osteoarthritis. *The Lancet*. 2019;393(10182):1745–59.
3. Loeser RF, Goldring SR, Scanzello CR, Goldring MB. Osteoarthritis: a disease of the joint as an organ. *Arthritis and rheumatism*. 2012;64(6):1697. [PubMed: 22392533]
4. Goldring SR, Goldring MB. Changes in the osteochondral unit during osteoarthritis: structure, function and cartilage–bone crosstalk. *Nature Reviews Rheumatology*. 2016;12(11):632–44. [PubMed: 27652499]
5. Jang S, Lee K, Ju JH. Recent Updates of Diagnosis, Pathophysiology, and Treatment on Osteoarthritis of the Knee. *International journal of molecular sciences*. 2021;22(5):2619. [PubMed: 33807695]
6. Nalapko Y, Klokol D, Lakey JR, et al. Novel Bioregenerative Options for Chondrocyte Restoration in Osteoarthritis. *Stem Cells Regen Med*. 2022;6(1):1–8.
7. Li X, Majumdar S. Quantitative MRI of articular cartilage and its clinical applications. *Journal of Magnetic Resonance Imaging*. 2013;38(5):991–1008. [PubMed: 24115571]
8. Eckstein F, Collins J, Nevitt M, Lynch J, Kraus V, Katz J, et al. Brief report: cartilage thickness change as an imaging biomarker of knee osteoarthritis progression: data from the Foundation for the National Institutes of Health Osteoarthritis Biomarkers Consortium. *Arthritis & rheumatology*. 2015;67(12):3184–9. [PubMed: 26316262]
9. Wirth W, Hunter D, Nevitt M, Sharma L, Kwok C, Ladel C, et al. Predictive and concurrent validity of cartilage thickness change as a marker of knee osteoarthritis progression: data from the Osteoarthritis Initiative. *Osteoarthritis and cartilage*. 2017;25(12):2063–71. [PubMed: 28838858]
10. Buck R, Wyman B, Le Graverand MPH, Hudelmaier M, Wirth W, Eckstein F, et al. Osteoarthritis may not be a one-way-road of cartilage loss—comparison of spatial patterns of cartilage change between osteoarthritic and healthy knees. *Osteoarthritis and Cartilage*. 2010;18(3):329–35. [PubMed: 19948267]
11. Wijayaratne SP, Teichtahl A, Wluka AE, Hanna F, Bell R, Davis SR, et al. The determinants of change in patella cartilage volume—a cohort study of healthy middle-aged women. *Rheumatology*. 2008;47(9):1426–9. [PubMed: 18641040]
12. Cicuttini F, Wluka A, Wang Y, Stuckey S. The determinants of change in patella cartilage volume in osteoarthritic knees. *The Journal of rheumatology*. 2002;29(12):2615–9. [PubMed: 12465162]

13. Cicuttini F, Hankin J, Jones G, Wluka A. Comparison of conventional standing knee radiographs and magnetic resonance imaging in assessing progression of tibiofemoral joint osteoarthritis. *Osteoarthritis and cartilage*. 2005;13(8):722–7. [PubMed: 15922634]
14. Buck R, Wirth W, Dreher D, Nevitt M, Eckstein F. Frequency and spatial distribution of cartilage thickness change in knee osteoarthritis and its relation to clinical and radiographic covariates—data from the osteoarthritis initiative. *Osteoarthritis and cartilage*. 2013;21(1):102–9. [PubMed: 23099212]
15. Cotofana S, Buck R, Wirth W, Roemer F, Duryea J, Nevitt M, et al. Cartilage thickening in early radiographic knee osteoarthritis: A within-person, between-knee comparison. *Arthritis care & research*. 2012;64(11):1681–90. [PubMed: 22556039]
16. Eckstein F, Wirth W, Lohmander L, Hudelmaier M, Frobell R. Five-year followup of knee joint cartilage thickness changes after acute rupture of the anterior cruciate ligament. *Arthritis & rheumatology*. 2015;67(1):152–61. [PubMed: 25252019]
17. Iriundo C, Liu F, Calivà F, Kamat S, Majumdar S, Padoia V. Towards understanding mechanistic sub-groups of osteoarthritis: 8-year cartilage thickness trajectory analysis. *Journal of Orthopaedic Research*. 2021;39(6):1305–17. [PubMed: 32897602]
18. Babel H, Omoumi P, Andriacchi TP, Jolles BM, Favre J. New insight on the subchondral bone and cartilage functional unit: Bone mineral density and cartilage thickness are spatially correlated in non-osteoarthritic femoral condyles. *Osteoarthritis and Cartilage Open*. 2020;2(3):100079. [PubMed: 36474682]
19. Shah RF, Martinez AM, Padoia V, Majumdar S, Vail TP, Bini SA. Variation in the thickness of knee cartilage. The use of a novel machine learning algorithm for cartilage segmentation of magnetic resonance images. *The Journal of arthroplasty*. 2019;34(10):2210–5. [PubMed: 31445869]
20. Le Graverand MPH, Buck R, Wyman B, Vignon E, Mazzuca S, Brandt K, et al. Subregional femorotibial cartilage morphology in women—comparison between healthy controls and participants with different grades of radiographic knee osteoarthritis. *Osteoarthritis and cartilage*. 2009;17(9):1177–85. [PubMed: 19341831]
21. Favre J, Scanlan SF, Erhart-Hledik JC, Blazek K, Andriacchi TP. Patterns of femoral cartilage thickness are different in asymptomatic and osteoarthritic knees and can be used to detect disease-related differences between samples. *Journal of biomechanical engineering*. 2013;135(10):101002. [PubMed: 23722563]
22. Favre J, Erhart-Hledik JC, Blazek K, Fasel B, Gold GE, Andriacchi TP. Anatomically standardized maps reveal distinct patterns of cartilage thickness with increasing severity of medial compartment knee osteoarthritis. *Journal of orthopaedic research*. 2017;35(11):2442–51. [PubMed: 28233332]
23. Peterfy CG, Schneider E, Nevitt M. The osteoarthritis initiative: report on the design rationale for the magnetic resonance imaging protocol for the knee. *Osteoarthritis and cartilage*. 2008;16(12):1433–41. [PubMed: 18786841]
24. Kohn MD, Sassoon AA, Fernando ND. Classifications in brief: Kellgren-Lawrence classification of osteoarthritis. *Clinical Orthopaedics and Related Research*[®]. 2016;474(8):1886–93. [PubMed: 26872913]
25. Morales Martinez A, Caliva F, Flament I, Liu F, Lee J, Cao P, et al. Learning osteoarthritis imaging biomarkers from bone surface spherical encoding. *Magnetic resonance in medicine*. 2020;84(4):2190–203. [PubMed: 32243657]
26. Morales AG, Lee JJ, Caliva F, Iriundo C, Liu F, Majumdar S, et al. Uncovering associations between data-driven learned qMRI biomarkers and chronic pain. *Scientific reports*. 2021;11(1):1–14. [PubMed: 33414495]
27. Lombaert H, Grady L, Polimeni JR, Cheriet F. FOCUSR: feature oriented correspondence using spectral regularization—a method for precise surface matching. *IEEE transactions on pattern analysis and machine intelligence*. 2012;35(9):2143–60.
28. Besl PJ, McKay ND. Method for registration of 3-D shapes. In: *Sensor fusion IV: control paradigms and data structures*. vol. 1611. Spie; 1992. p. 586–606.

29. Iranpour-Boroujeni T, Li J, Lynch J, Nevitt M, Duryea J, Investigators O, et al. A new method to measure anatomic knee alignment for large studies of OA: data from the Osteoarthritis Initiative. *Osteoarthritis and cartilage*. 2014;22(10):1668–74. [PubMed: 25278076]
30. Jørgensen DR, Lillholm M, Genant HK, Dam EB. On subregional analysis of cartilage loss from knee MRI. *Cartilage*. 2013;4(2):121–30. [PubMed: 26069655]
31. Andriacchi TP, Mündermann A, Smith RL, Alexander EJ, Dyrby CO, Koo S. A framework for the in vivo pathomechanics of osteoarthritis at the knee. *Annals of biomedical engineering*. 2004;32(3):447–57. [PubMed: 15095819]
32. Chaudhari A, Briant PL, Bevill SL, Koo S, Andriacchi TP. Knee kinematics, cartilage morphology, and osteoarthritis after ACL injury. *Medicine and science in sports and exercise*. 2008;40(2):215–22. [PubMed: 18202582]
33. Silverwood V, Blagojevic-Bucknall M, Jinks C, Jordan J, Protheroe J, Jordan K. Current evidence on risk factors for knee osteoarthritis in older adults: a systematic review and meta-analysis. *Osteoarthritis and cartilage*. 2015;23(4):507–15. [PubMed: 25447976]
34. Faber S, Eckstein F, Lukasz S, Mühlbauer R, Hohe J, Englmeier KH, et al. Gender differences in knee joint cartilage thickness, volume and articular surface areas: assessment with quantitative three-dimensional MR imaging. *Skeletal radiology*. 2001;30(3):144–50. [PubMed: 11357452]
35. Hitt K, Shurman JR, Greene K, McCarthy J, Moskal J, Hoeman T, et al. Anthropometric measurements of the human knee: correlation to the sizing of current knee arthroplasty systems. *JBJS*. 2003;85(suppl 4):115–22.
36. O'Connor MI. Osteoarthritis of the hip and knee: sex and gender differences. *Orthopedic Clinics*. 2006;37(4):559–68. [PubMed: 17141013]
37. Richmond RS, Carlson CS, Register TC, Shanker G, Loeser RF. Functional estrogen receptors in adult articular cartilage: Estrogen replacement therapy increases chondrocyte synthesis of proteoglycans and insulin-like growth factor binding protein 2. *Arthritis & Rheumatism: Official Journal of the American College of Rheumatology*. 2000;43(9):2081–90.
38. Mezhev V, Ciccutini FM, Hanna FS, Brennan SL, Wang Y, Urquhart DM, et al. Does obesity affect knee cartilage? A systematic review of magnetic resonance imaging data. *Obesity reviews*. 2014;15(2):143–57. [PubMed: 24118701]
39. Blazek K, Favre J, Asay J, Erhart-Hledik J, Andriacchi T. Age and obesity alter the relationship between femoral articular cartilage thickness and ambulatory loads in individuals without osteoarthritis. *Journal of Orthopaedic Research*. 2014;32(3):394–402. [PubMed: 24281940]
40. Sowers MR, Karvonen-Gutierrez CA. The evolving role of obesity in knee osteoarthritis. *Current opinion in rheumatology*. 2010;22(5):533. [PubMed: 20485173]
41. Sharma L, Lou C, Cahue S, Dunlop DD. The mechanism of the effect of obesity in knee osteoarthritis: the mediating role of malalignment. *Arthritis & Rheumatism: Official Journal of the American College of Rheumatology*. 2000;43(3):568–75.
42. Moyer RF, Birmingham TB, Chesworth BM, Kean C, Giffin JR. Alignment, body mass and their interaction on dynamic knee joint load in patients with knee osteoarthritis. *Osteoarthritis and cartilage*. 2010;18(7):888–93. [PubMed: 20417288]
43. Lee R, Kean WF. Obesity and knee osteoarthritis. *Inflammopharmacology*. 2012;20(2):53–8. [PubMed: 22237485]
44. Lohmander LS, De Verdier MG, Roloff J, Nilsson PM, Engström G. Incidence of severe knee and hip osteoarthritis in relation to different measures of body mass: a population-based prospective cohort study. *Annals of the rheumatic diseases*. 2009;68(4):490–6. [PubMed: 18467514]
45. Holliday K, McWilliams D, Maciewicz R, Muir K, Zhang W, Doherty M. Lifetime body mass index, other anthropometric measures of obesity and risk of knee or hip osteoarthritis in the GOAL case-control study. *Osteoarthritis and Cartilage*. 2011;19(1):37–43. [PubMed: 21044695]
46. Karvonen R, Negendank W, Teitge R, Reed A, Miller P, Fernandez-Madrid F. Factors affecting articular cartilage thickness in osteoarthritis and aging. *The Journal of rheumatology*. 1994;21(7):1310–8. [PubMed: 7966075]
47. Pelletier JP, Raynauld JP, Berthiaume MJ, Abram F, Choquette D, Haraoui B, et al. Risk factors associated with the loss of cartilage volume on weight-bearing areas in knee osteoarthritis patients

assessed by quantitative magnetic resonance imaging: a longitudinal study. *Arthritis research & therapy*. 2007;9(4):1–11.

48. Price LL, Harkey MS, Ward RJ, MacKay JW, Zhang M, Pang J, et al. Role of magnetic resonance imaging in classifying individuals who will develop accelerated radiographic knee osteoarthritis. *Journal of Orthopaedic Research*[®]. 2019;37(11):2420–8. [PubMed: 31297900]
49. Maldonado M, Nam J. The role of changes in extracellular matrix of cartilage in the presence of inflammation on the pathology of osteoarthritis. *BioMed research international*. 2013 Aug 28;2013.

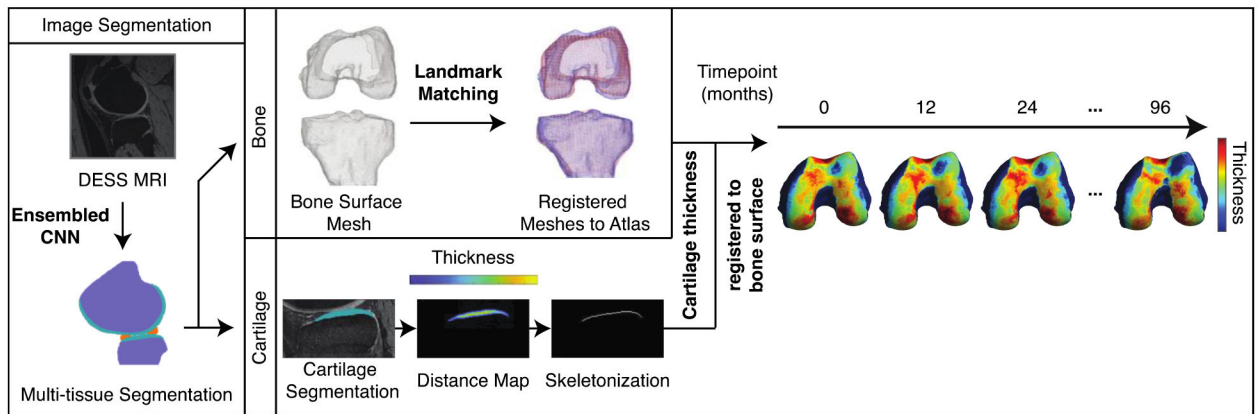


Figure 1: Overview of image processing pipeline.

A segmentation model ensemble was used to automatically segment bone and cartilage in sagittal slices of knee MRI volumes. Bone meshes were registered to a reference bone surface. Per sagittal slice, a Euclidean distance transform and skeletonization was performed on cartilage segmentations. The distance map was projected to the underlying bone mesh to obtain a dense cartilage thickness map for each knee volume at each time point. Implementation details can be found in Iriondo et al., 2020.¹⁷

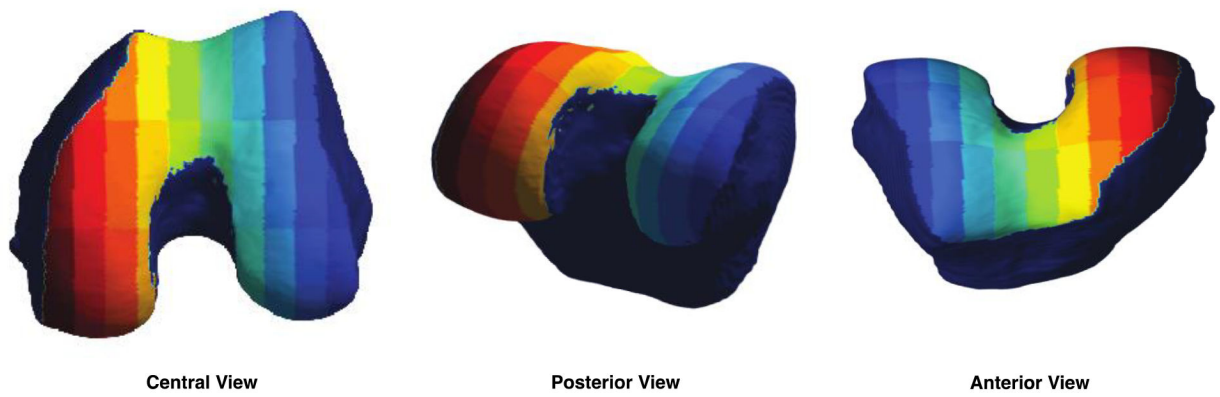


Figure 2: Cartilage Parcellation Atlas.

An atlas was created by dividing the three-dimensional reference cartilage mask into 27 subregions (4–5 subregions per compartment), each represented by a different color.

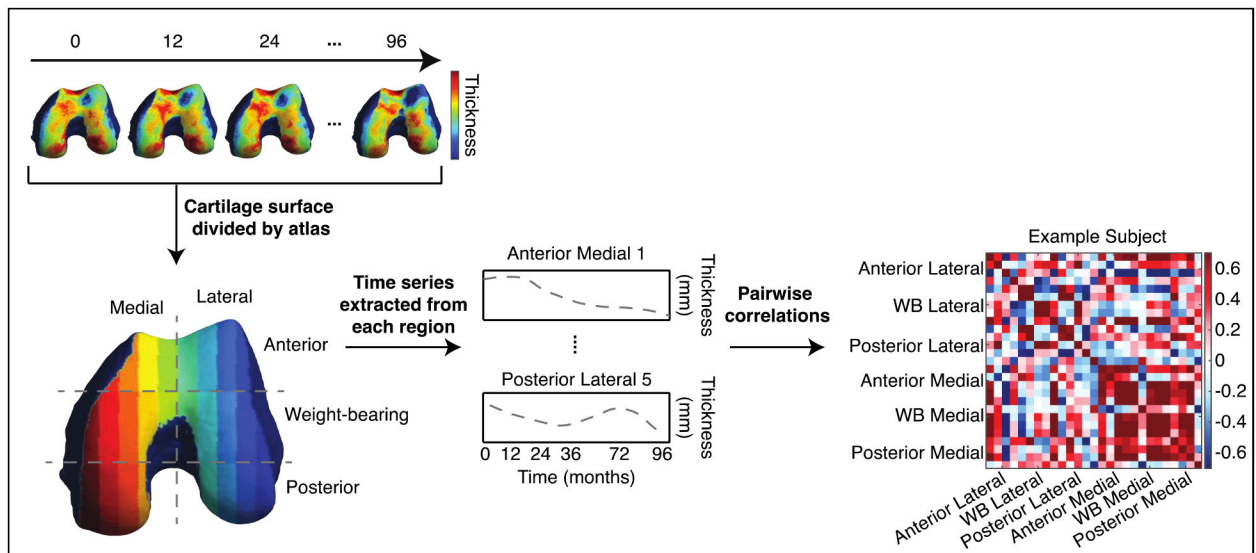


Figure 3: Schematic of connectome generation.

Cartilage thickness values at all vertices within each subregion of the cartilage atlas were averaged to obtain a single value per subregion. This was performed at all time points to obtain cartilage thickness trajectories for all subregions. Pearson correlation coefficient r was used to represent the similarity between each pairwise combination of time series, resulting in a symmetric correlation matrix (connectome) for each knee. Each row/column entry in the connectome represents the correlation between the thickness trajectories of a pair of the 27 subregions. Every labeled compartment in the connectome contains 4–5 subregions.

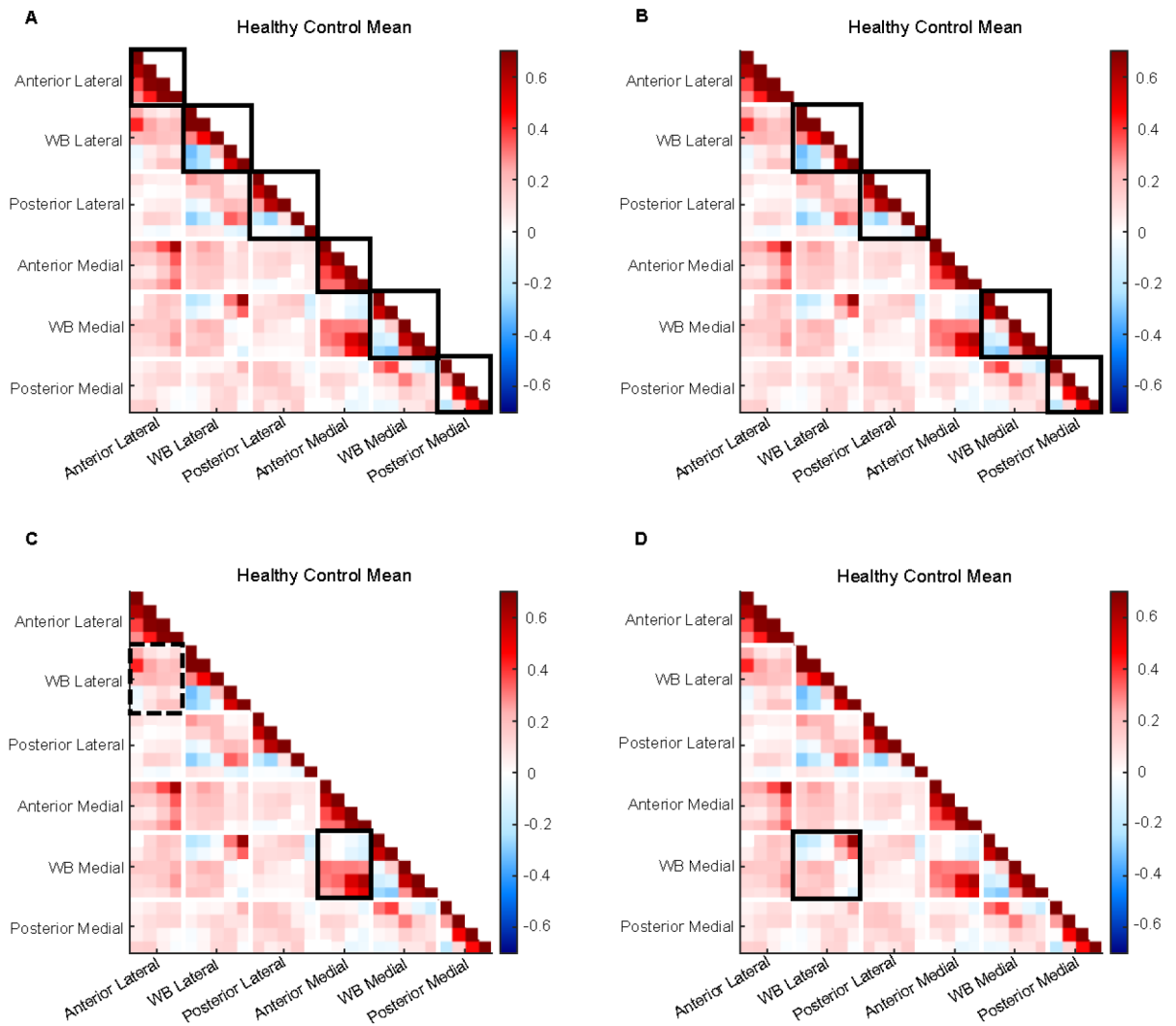


Figure 4: Illustration of key descriptive features of average control connectome.

A) Intracorrelations (solid boxes) are generally stronger than intercorrelations (all else). B) Weight-bearing and posterior regions (solid boxes) have strong positives but also weak to moderate negatives. C) Associations between anterior and weight-bearing compartments are stronger in medial (solid) than lateral (dashed) sides. D) Consistent anticorrelation pattern observed between medial and lateral weight-bearing regions (solid box).

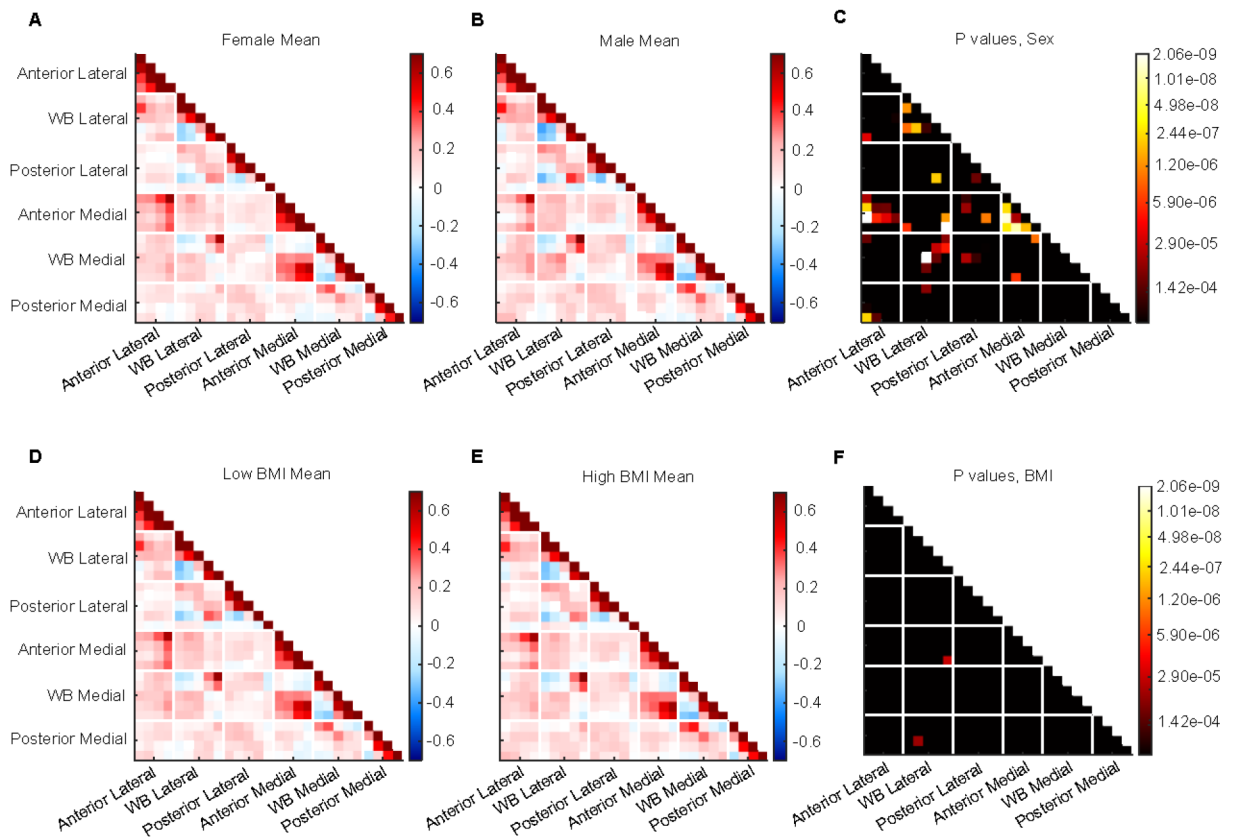


Figure 5: Population differences within control group.

A) Mean connectome for female subjects. B) Mean connectome for male subjects. C) P-value matrix comparing male and female mean connectomes. D) Mean connectome for subjects with a BMI below 30. E) Mean connectome for subjects with BMI \geq 30. F) P-value matrix comparing mean connectomes for high and low BMI subjects.

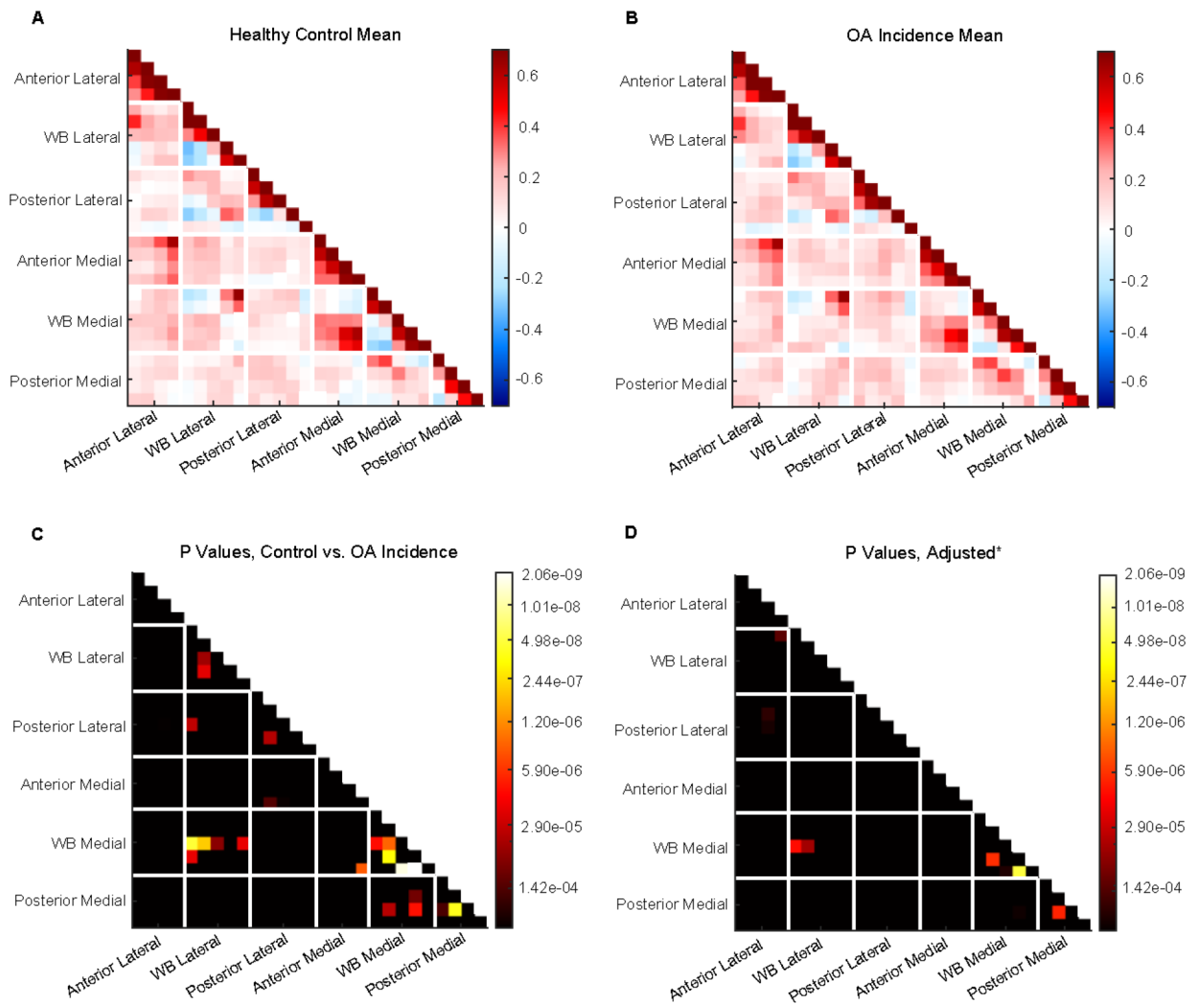


Figure 6: Comparison between control and OA incidence groups.

A) Mean connectome for control group. B) Mean connectome for OA incidence group. C) P-value matrix comparing control and OA incidence groups. D) P-value matrix of partial correlation analysis comparing control and OA incidence groups while controlling for sex, BMI, and knee alignment.

**Table 1:
Demographics of Control and OA Incidence subject groups.**

Continuous variables (age, BMI) shown as mean (standard deviation). Categorical variables (sex, knee alignment) shown as raw count (% of total). Varus and valgus data (italicized) calculated on a subset of knees (454 in Control Group, 229 in OA Incidence Group).

	Control (n = 1186)	OA Incidence (n = 232)
Sex = Female	641 (54%)	163 (70%)**
Age [years]	58.7 (8.5)	59.6 (8.7)
BMI [kg/m ²]	27.1 (4.2)	28.7 (4.3)**
<i>Varus Alignment</i>	143 (31.5%)	57 (24.9%)*
<i>Valgus Alignment</i>	8 (1.8%)	10 (4.4%)*

* $p < .05$ and

** $p < 0.001$